Hindawi Publishing Corporation
Journal of Nanomaterials
Volume 2012, Article ID 713203, 7 pages
doi:10.1155/2012/713203

Research Article

Optical Characterization of Chemically Etched Nanoporous Silicon Embedded in Sol-Gel Matrix

A. S. Al Dwayyan,[1] M. Naziruddin Khan,[2] and M. S. Al Salhi[1]

[1] *Department of Physics and Astronomy, College of Science, King Saud University, P.O. Box 2455, Riyadh 11451, Saudi Arabia*
[2] *King Abdullah Institute for Nanotechnology (KAIN), King Saud University, P.O. Box 2455, Riyadh 11451, Saudi Arabia*

Correspondence should be addressed to M. Naziruddin Khan, mnkhan_phy@yahoo.com

Received 29 November 2011; Revised 29 December 2011; Accepted 30 December 2011

Academic Editor: Haibo Zeng

Nanoporous (NPs) silicon fabricated by chemical etching process in HF acid was first separated in tetrahydrofuran (THF) solvent and then incorporated into SiO_2 matrix. The matrix was prepared by sol gel process in which dimethylformamide (DMF) was used as drying chemical control additive (DCCA) to form crack-free dried sample. We examined the optical properties of NPs in three medium which are solvent, sol, and dried sol gel. Our observations reveal that absorption spectra of NPs silicon in THF are modified with respect to the spectra in sol gel. Significant stability in PL of NPs silicon in the sol gel is observed. Influence of matrix environment on peaks of NPs is also discussed. Surface morphology is characterized by field emission scanning electron microscopy (FESEM) which shows that the NPs silicon in THF is similar to the sol gel but becomes aggregation particle to particle. Presence of Si nanoparticles in THF and sol is confirmed by Transmission electron microscopy (TEM). The NPs silicons have mono dispersive and high crystalline nature with spherical shape of around 5 nm in sizes.

1. Introduction

Nanocrystals (NCs), also known as quantum dots (QDs) are special class of semiconductor materials because small sizes behave differently in their properties. Porous silicon (PSi) is considered as one of the NCs and was first discovered by Uhlir [1] but its photoluminescence (PL) properties remained unnoticed until 1990, when the luminescence properties were reported by Canham [2]. Strong visible luminescence from porous silicon (PSi) at room temperature has initiated new ideas for Si-based optoelectronics. Due to its particular structure and surface reactivity, porous silicon has stimulated much research for many applications in different fields such as light emitting diodes, optical sensors, biomedical applications, interference filters, and wave guides [2]. Since then, silicon nanoparticles was made by a variety of techniques, that is, physically or chemically [3–7]. Most techniques indicate that silicon nanoparticles exhibit efficient room-temperature luminescence in visible range. Its spectrum was characterized by three main features; a blue band, the broad red orange band, and an infrared band peaked at roughly 1 ev [8, 9]. On the other hand, a great variety of nanoparticles are currently used for bioanalysis including quantum dots [10] and silica nanoparticles [11]. The availability of PSi discrete size and distinct emission in the red, green, and blue range is also important for biomedical tagging [12, 13]. Due to the nontoxic properties of Si and Si oxide, the redox behavior of silicon nanoparticles (Si-nps) produced by laser ablation in colloidal was studied after addition of noble metal salts [14] which are potential applications in pollution.

PSi features are much less understood in terms of their fundamental photophysics than the particles made from direct gap semiconductors [15]. The incorporation or fabrication of nanometer-sized crystalline semiconductor into glass matrices remains an area of extensive interest [16–19]. These composite materials are well known and play an important role with respect to fast optical switching and optical nonlinearity [20]. The sol-gel process is widely realized as an ideal media for nanoparticles due to its

unique advantages such as low temperature processing, high homogeneity of final products, and its capability to generate materials with controlled surface properties and pore structures [21, 22]. The technique for synthesis of semiconductor nanoparticles stabilized within the solid silica matrices is more advantageous for understanding the properties of nanomaterials.

Incorporation of Si nanocrystallites extracted from porous Si into a silica sol-gel matrix was reported where the emission peaks of Si nanoparticles doped sol-gel changes as the concentration of nanoparticles increases [23, 24]. PL stability of NPs silicon in sol-gel environment is still problem since sol-gel host depends on various factors, that is, natures of precursor, composition, solvents, catalyst, and pH value. In this connection, our group reported the effect of solvent and cosolvent on molecule doped-sol-gel matrix [25, 26].

In spite of many attempt to describe the PL properties of Si nanoparticles produced by various techniques, a proper assignment of individual emission features of the Si nanoparticle-doped sol-gel in terms of optical, thermal, mechanical properties and is still limited. Earlier our work reported on the basic optical properties of Si nanocrystals powder in sol-gel matrix and discussed their PL stability [27, 28]. The aim of this present work is to understand the PL properties of the nanoporous silicon fabricated by chemical etching process in sol-gel matrix. Therefore, we studied the absorption and PL spectral changes caused by the sol-gel environment. We report an interesting behavior of PL spectra of NPs sol-gel combination resulting in an active material which may be used in optical applications.

2. Experimental

Synthesis of luminescent porous silicon is performed by anodization process in hydrofluoric acid- (HF-) based solutions with electrical source [7, 29]. In this work, we fabricated red emitting nanoporous silicon by a simple chemical etching process in a highly catalyst solution of 40% HF, hexachloroplatinic (IV) acid (H_2PtCl_6), deionised water and etchant solution of methanol, as well as HF and 30% H_2O_2 to produce crystalline Si into ultrasmall nanoparticles. Because HF is highly reactive with silicon oxide, H_2O_2 catalyzes the etching, producing smaller particles. Moreover, the oxidative nature of the peroxides produces high chemical and electronic quality samples. Single P-type boron-doped Si wafers (100, 1–10 ohm) were cut into small rectangular pieces 1×10 cm in area, ultrasonically cleaned with acetone, dried with N_2 gas and put in a polypropylene tank-filled catalyst solution about 15 min. The samples were then rinsed with deionized water and dried in blowing N_2 gas. The subsequent chemical etching was made for 15 s of each sample in the etchant solution. Finally, the etched wafers were rinsed in isopropanol each time after the etching and dried slowly with N_2 gas. The pulverized wafer pieces were transferred into a small disk filed with THF and then sonicated in an ultrasound bath to disperse the Si nanoparticles. Samples were centrifuged to screen the particles. In order to make sure the presence of nanoparticles, sample was exposed to an UV lamp at 365 nm.

Tetraethylorthosilance (TEOS, Aldrich, 98%) was used as the inorganic precursor. The sols were obtained from hydrolysis and polycondensation of TEOS using THF as solvent, dimethylformamide (DMF) as drying chemical control additive (DCCA), as well as distilled water and nitric acid as catalyst. The molar ratio of TEOS : THF : DMF : Water : Nitric acid in the sample was [1 : 1.5 : 0.5 : 1 : 0.01], respectively. DMF was added to the TEOS/THF solution under stirring after 40 minutes in an open glass beaker. The water/nitric acid mixture was added to the solution and stirred about 30 minutes. About 4 mL of nanoporous silicon THF solution was introduced in the 8 mL of sol and 5 min ultrasonic treatment followed. The final solution was kept at room temperature for few week in quartz cuvettes and cylindrical polystyrene tubes to achieve solidification. Measurements of absorption, emission, and excitation spectra were made in UV-Visible spectrophotometer (Perkin Elmer Lamda 40) and Luminescence spectrophotometer (LS 45 Perkin Elmer), respectively. SEM image was obtained by Field emission scanning electron microscope (JEOL, JSM-6380LA). TEM image was taken in an HRTEM (Jeol-JEM2100F). The resulting samples were checked to make sure that NPs were luminescing light to the naked eyes under an UV lamp (model XX15NF, Spectroline USA).

3. Results and Discussion

The optical absorption and emission of nanoporous silicon in all medium were taken at room temperature. The measured PL emission was excited with 265, 355, and 365 nm in all samples and compared. The red luminescence NPs embedded sol-gel samples are seen under UV excitation (365 nm) as shown in Figures 1(a) and 1(b) and found to be stable.

3.1. Absorption Spectra. Figure 2 shows the comparison absorption spectra of NPs silicon in THF, sol and dried sol-gel matrix. It exhibits two peaks at 250 nm and 320 nm in THF which corresponds to the peaks observed at 260 nm and 325 when the NPs silicon was embedded in sol-gel matrix, but peaks of NPs silicon do not change from sol to gel solid except the absorbance slightly decays and both feature become merge as seen in Figure 2 (curve (i) (a, b), curve (ii) (a, b), and curve (iii) (a, b)) with respect to the feature of THF. Effects on absorbance suggest that internal light scattering within matrix can be expected due to phase change from sol-solid. Indeed, the optical response of nanoporous silicon reflects the sum of the scattering and absorption. However, the change in spectra of NPs from solvent to sol-gel is attributed to the cause of matrix environment. The scattering needs to be taken into consideration in sol-gel solid environment since the transition of sol liquid to solid phase influences to the distribution of native nanoporous silicon. The absorption peak positions of NPs in THF, sol and sol-gel solid are listed in Table 1. Our earlier work on the silicon nanocrystallines powder in sol-gel obtained as similar to present results [28]. On the other hand, from the theoretical point of view reported in [30] that significant influences of the matrix material on the electronic

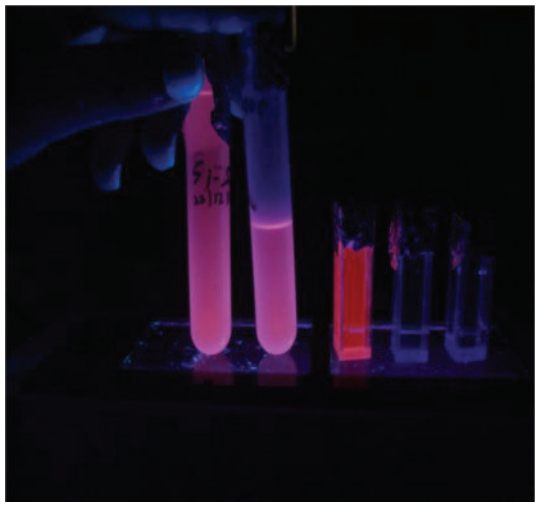

(a)

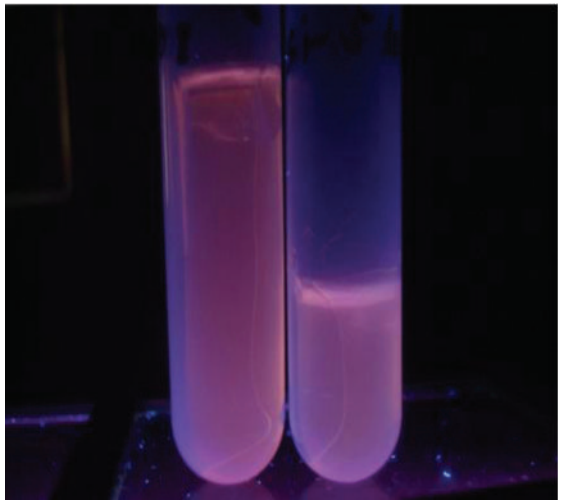

(b)

Figure 1: Digital images of red emitting NPs Silicon in (a) sol and (b) dried sol-gel in a cylindrical tube under UV lamp excited at 365 nm.

Table 1: Absorption, emission, and excitation of NPs Si in THF, sol and sol-gel solid.

Measurement	THF	Sol	Sol-gel matrix (solid)
Absorption peaks	250 nm	260 nm	260 nm
	320 nm	320 nm	325 nm
	633 nm	642 nm	605 nm
Emission peaks	628 nm	642 nm	605 nm
	628 nm	642 nm	605 nm
Excitation peaks	258 nm	250 nm	252 nm
	303 nm	333 nm	346 nm

confinement and energies level were found reduced in presence of SiO_2 matrix.

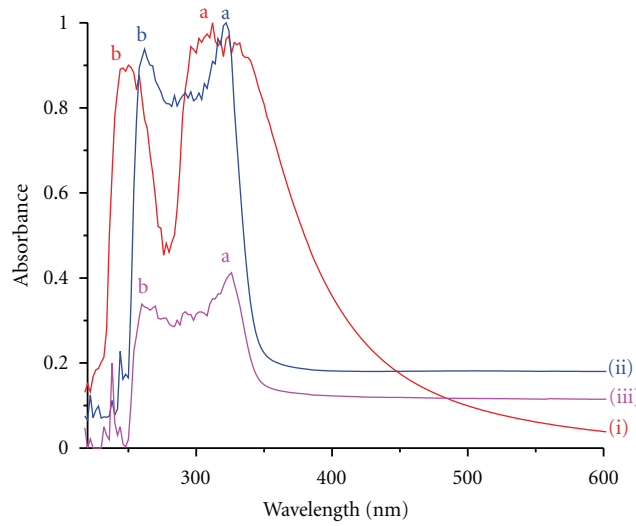

Figure 2: Absorption spectra of NPs silicon in (i) THF (ii) sol and (iii) sol-gel solid.

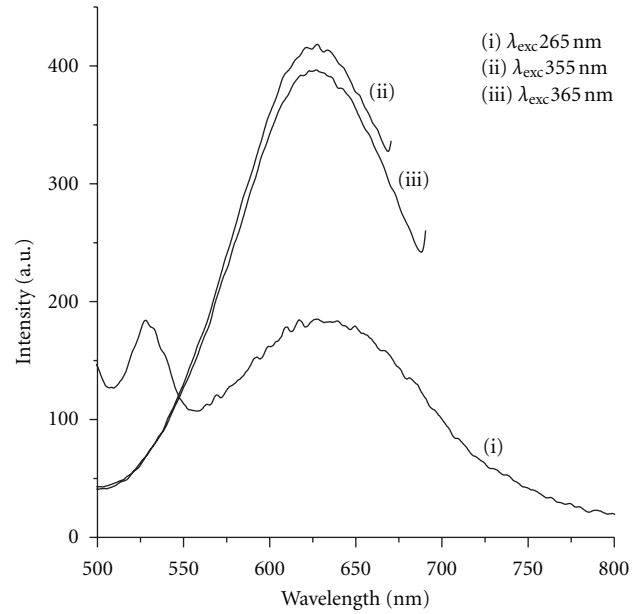

Figure 3: Emission spectra of NPs silicon in THF.

The origin of 325 nm absorption band may consider to the work reported [31] that the optical absorption of Si at 320 nm (4 ev) relatively size nanocrystals (d = 3.7–10 nm) is associated with direct transition Γ_{25}-Γ_2. While the second absorption band at 250 nm may be related to the work of Ma et al. [32] found that the absorption of nc-Si in the range of 1.5–3.0 eV is due to indirect band to band transition but the first direct band of Si is 3.4 eV.

3.2. Emission Spectra. Figures 3, 4, and 5 which present typical luminescence spectra of nanoporous silicon in THF, sol and sol-gel solid obtained at room temperature. These spectra were obtained by exciting the NPs samples using

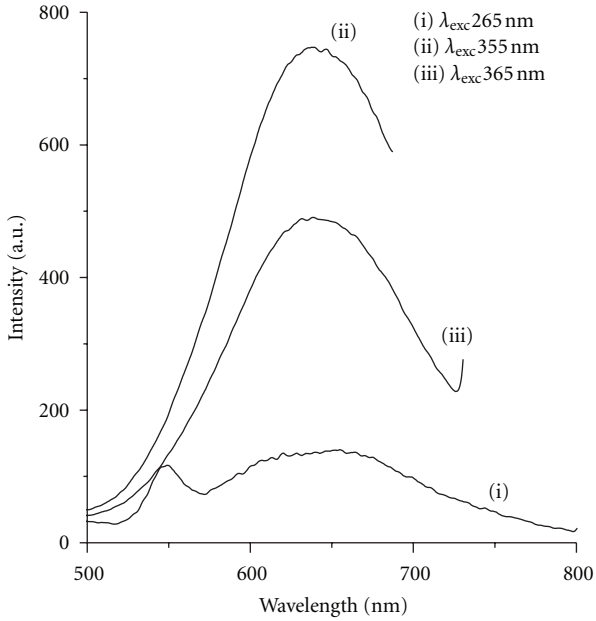

Figure 4: Emission spectra of NPs in sols (liquid) Such solvent may help the intensity variation of NPs Si in sol-gel host. However, DMF used as DCCA may help to form better sol-gel quality in terms of monolithicity, transparency, low density, and control the rate of evaporation during aging. The peak positions of NPs Si in THF, sol and sol-gel solid are summarized in Table 1.

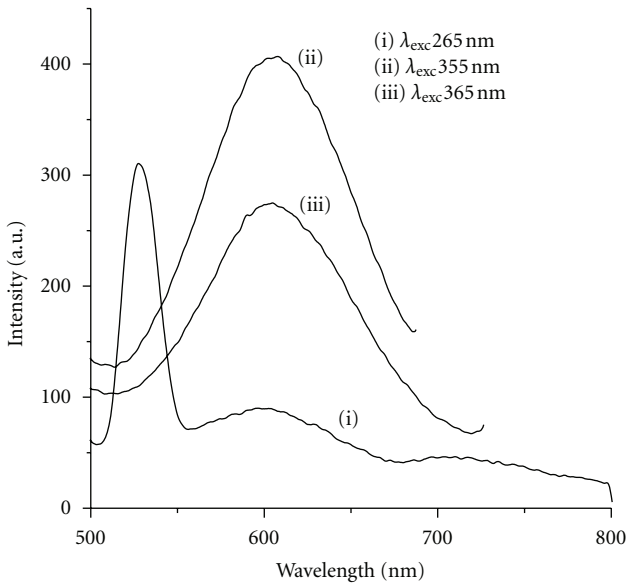

Figure 5: Emission spectra of NPs in sol-gel solid.

three different wavelengths (265, 355, and 365 nm) in the range 500–800 nm, respectively. The observed band shapes of all samples are similar, but a small red shift of the doped sol-gel (sol state) with respect to solvent and its blue shift after solidified the sol-gel can probably be attributed to matrix environmental effect. Observations evidence that

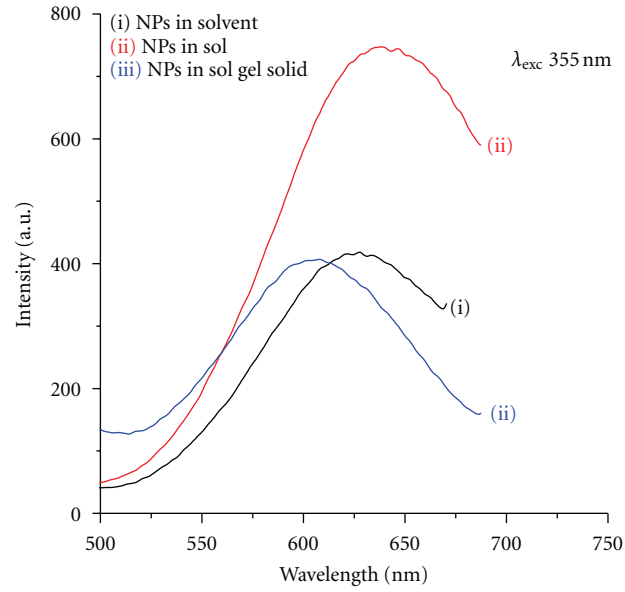

Figure 6: Emission of NPs in THF-Sol-Solid under excitation 355 nm.

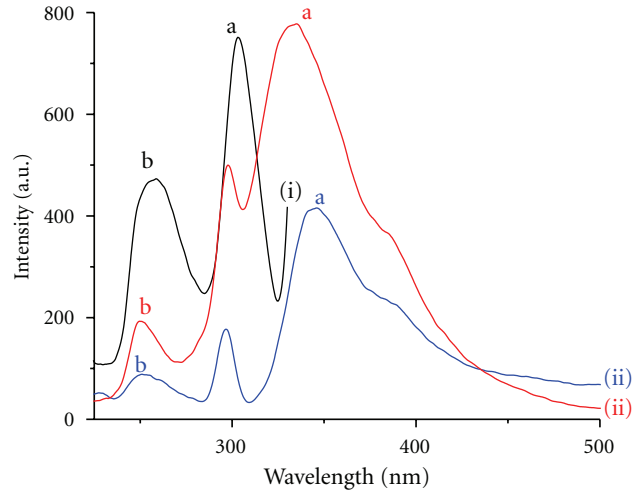

Figure 7: Excitation spectra of NPs silicon in (i) THF, sol (i) and (ii) sol-gel solid.

luminescence intensity of the NPs are dependence of excitation wavelengths indicating that increase in intensity with the excitation increases up to 355 nm and then decays as shown in Figures 3–5 (curve (i), (ii), (iii)), respectively. The best PL intensity is pronounced at the excitation 355 nm. These PL bands of NPs THF, sol, and solid for the 355 nm excitation is compared as shown in Figure 6 (curve (i), (ii), (iii)) that clearly exhibit more intense the emission light from NPs Si doped sol than the corresponding to THF and sol-gel solid. It is also evident that no significant change is noticed in the emission positions with the variation of excitation wavelength, but as earlier reported [33, 34] by varying the excitation energy, luminescence crystallites of different sizes are photoexcited and emission band shifts

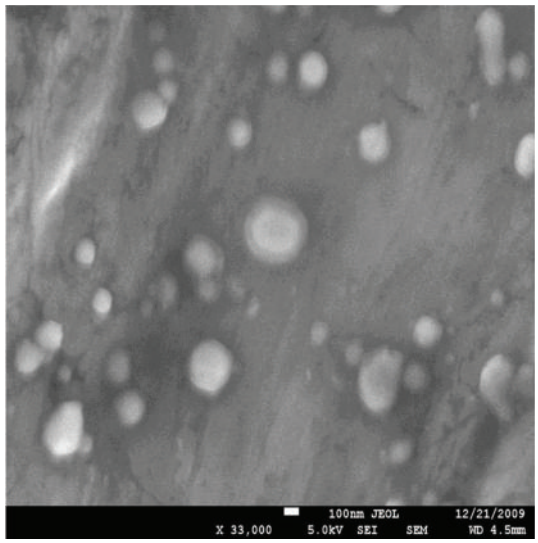

(a)

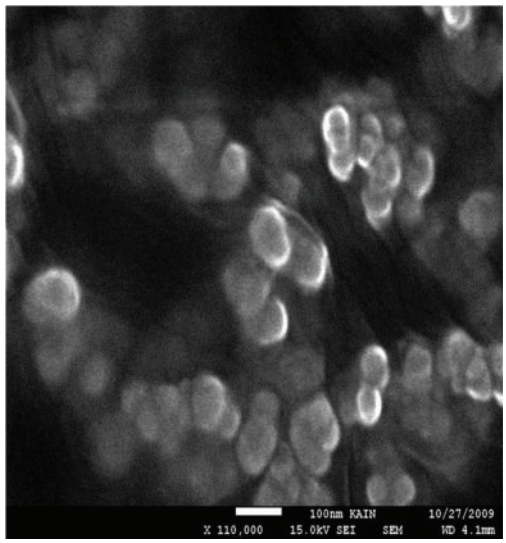

(b)

Figure 8: FESEM image of NPs silicon in (a) THF (b) sol-gel solid.

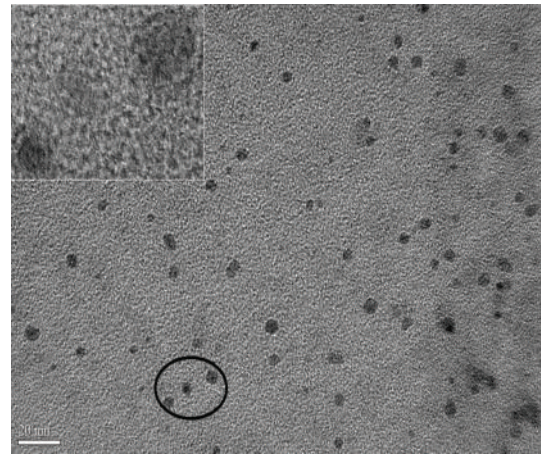

(a)

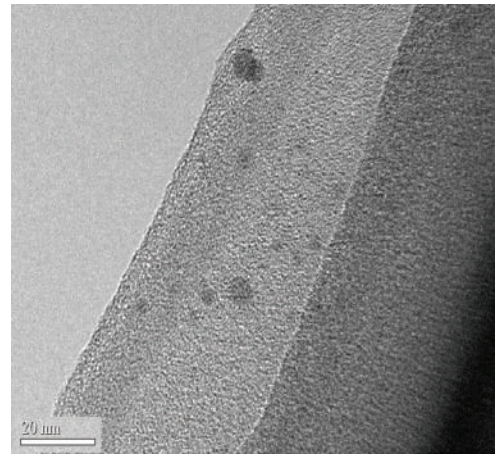

(b)

Figure 9: HRTEM images of NPs silicon in (a) THF (b) sol-gel at 20 nm scale. The inset shows the lattice pattern of nanoparticles.

accordingly. It may stress that nonuniformity of NPs Si distribution in the matrix environment; role of interface between NPs Si/SiO_2 [35] would induce effects on intensities. Since sol-gel matrix-derived SiO_2 is an oxygen environment which can cause a substantial decrease in luminescence, the change of native NPs silicon in sol-gel during the extraction of liquid (aging) may influence to luminescence intensities. In general, evaporation of THF solvent from sol-gel is faster and also less quenching in comparison to other solvents [26].

Although low Si concentration was employed in present studies, the broad emission band observed with better distinctly than earlier result [24]. This could be probably due to the fact that luminescence was less quenched with THF solvent. It is reported elsewhere [23] that using the ethanol as solvent in sol-gel with Si nanoparticles leads to quenching.

Further, Fojtik and Henglein [36] studied the suspension of the Si nanoparticles causing a shift in the PL properties. It is true that rapid thermal oxidations of the emitting particles can be influenced with the peak of PL emission [37]. On contrary, the PL of low-density PSi nanoparticles monolith for various excitation wavelengths was observed to be changed [24]. They found that the blue band shifts toward red as the excitation energy was reduced.

3.3. Excitation Spectra. Figure 7 shows the comparison excitation spectra of nanoporous silicon in THF, sol and sol-gel-derived solid, respectively. The excitation peaks in all medium are in fact identical compared in accordance with absorption spectra.

The significant red shift with the intensively excitation peaks of NPs-doped sol (at 333) and solid (at 342 nm) corresponding to THF (303 nm) is observed, respectively, as seen in Figure 6 (curves (i), (ii), (iii)). On the other hand, a small blue shift with weak peaks is followed. The spectrum

of NPs sol-gel is wider than that of THF. These effects on excitation spectra of NPs resemblance to absorption and PL which can be attributed to the influence of matrix. The facts that excitation peak positions of NPs THF, sol, and solid are closely exhibited to the absorption peaks observed at 250 and 320 nm. The comparison absorption and excitation peaks are listed in Table 1. Overall, our observations suggest that optical properties of nanoporous silicon in sol-gel are fairly stable and can be produced crack free transparent sample.

Thus luminescence property of NP Si-doped sol-gel depends on the physical states. Figure 8 shows the field emission SEM plane view images of the NPs Si THF solution and sol-gel matrix. The particle distribution of THF suspension is approximately uniform with different pore sizes as shown Figure 8(a). This surface morphology has a difference with the surface-dried NPs-doped sol-gel which is seen in Figure 8(b), in which distributions of nanoparticles in sol-gel become nonuniform whereas some are more dense at lower part of image and aggregate particle to particle.

The encapsulated particles are nearly spherical and can be classified into a small number. It may be possible that NPs Si are closer due to shrinkage of sol-gel structure on the evaporation of liquid from the sol after solidification. Therefore, the existence of variation in PL intensity of dried sol-gel can be attributed to this factor.

Figure 9 shows the HRTEM image of the NPs Si taken by dropping the THF solution and sol onto a carbon-coated TEM grid. Most of the Si nanoparticles are uniformly dispersive and have sizes around more or less 5 nm. The inset of Figure 9(a) displays the lattice lines of the selected area of Si nanoparticles, indicating highly crystalline nature. Although majority of the NPs Si are 5 nm in diameter but there is some small size present less than 5 nm. Presence of few NPs silicon in sol-gel is confirmed as seen in Figure 9(b).

4. Conclusion

Chemically etched NPs silicons were successfully incorporated in sol-gel matrix. Optical properties of NPs silicon-doped sol-gel were studied under different condition. PL property of NPs sol-gel combination is found to be significantly stable and also obtained crack-free dried product. Present results reveal that chemical compositions involved in sol-gel process are a key factor to stabilize the NPs silicon. A proper addition of higher concentration of silicon nanoparticles into such transparent inert sol-gel medium may possibly be converted into active material for optical amplification. It concludes that sol-gel matrix prepared at low temperature is found to be a suitable host for silicon nanoparticles without altering the basic properties of the dopant. More study of the NPs Si in sol-gel matrix is still underway under various conditions to better understanding.

Acknowledgments

The authors gratefully acknowledge National Plan for Science and Technology (NPST) of King Saud University, for financial support under (Grant no. 10NAN-1037-02).

References

[1] A. Uhlir Jr., "Electrolytic shaping of germanium and silicon," *The Bell System Technical Journal*, vol. 35, pp. 333–347, 1956.

[2] L. T. Canham, "Silicon quantum wire array fabrication by electrochemical and chemical dissolution of wafers," *Applied Physics Letters*, vol. 57, no. 10, pp. 1046–1048, 1990.

[3] J. L. Heinrich, C. L. Curtis, G. M. Credo, K. L. Kavanagh, and M. J. Sailor, "Luminescent colloidal silicon suspensions from porous silicon," *Science*, vol. 255, no. 5040, pp. 66–68, 1992.

[4] O. Schoenfeld, X. Zhao, J. Christen, T. Hempel, S. Nomura, and Y. Aoyagi, "Formation of Si quantum dots in nanocrystalline silicon," *Solid-State Electronics*, vol. 40, no. 1-8, pp. 605–608, 1996.

[5] J. P. Wilcoxon, G. A. Samara, and P. N. Provencio, "Optical and electronic properties of Si nanoclusters synthesized in inverse micelles," *Physical Review B*, vol. 60, no. 4, pp. 2704–2714, 1999.

[6] K. Hata, S. Yoshida, and M. Fujita, "Self-assembled monolayer as a template to deposit silicon nanoparticles fabricated by laser ablation," *The Journal of Physical Chemistry*, vol. 105, pp. 10842–10846, 2001.

[7] O. Akcakir, J. Therrien, G. Belomoin et al., "Detection of luminescent single ultrasmall silicon nanoparticles using fluctuation correlation spectroscopy," *Applied Physics Letters*, vol. 76, no. 14, pp. 1857–1859, 2000.

[8] L. Tysbeskov, J. U. V. Vanydeshev, and P. M. Faucet, "Blue emission in porous silicon: oxygen-related photoluminescence," *Physical Review B*, vol. 49, pp. 7821–7824, 1994.

[9] M. S. Brandt and M. Stutzmann, "Spin-dependent effects in porous silicon," *Applied Physics Letters*, vol. 61, no. 21, pp. 2569–2571, 1992.

[10] F. Pinaud, X. Michalet, L. A. Bentolila et al., "Advances in fluorescence imaging with quantum dot bio-probes," *Biomaterials*, vol. 27, no. 9, pp. 1679–1687, 2006.

[11] M. Qhobosheane, S. Santra, P. Zhang, and W. Tan, "Biochemically functionalized silica nanoparticles," *Analyst*, vol. 126, no. 8, pp. 1274–1278, 2001.

[12] T. J. Dougherty, "Photosensitizers: therapy and detection of malignant tumors," *Photochemistry and Photobiology*, vol. 45, no. 6, pp. 879–889, 1987.

[13] G. Belomoin, J. Therrien, A. Smith et al., "Observation of a magic discrete family of ultrabright Si nanoparticles," *Applied Physics Letters*, vol. 80, no. 5, p. 841, 2002.

[14] S. Yang, W. Cai, G. Liu, H. Zeng, and P. Liu, "Optical study of redox behavior of silicon induced by laser ablation in liquid," *Journal of Physical Chemistry C*, vol. 113, no. 16, pp. 6480–6484, 2009.

[15] L. Brus, "Luminescence of silicon materials: chains, sheets, nanocrystals, nanowires, microcrystals, and porous silicon," *Journal of Physical Chemistry*, vol. 98, no. 14, pp. 3575–3581, 1994.

[16] S. S. Yao, C. Karaguleff, A. Gabel, R. Fortenberry, C. T. Seaton, and G. I. Stegeman, "Ultrafast carrier and grating lifetimes in semiconductor-doped glasses," *Applied Physics Letters*, vol. 46, no. 9, pp. 801–802, 1985.

[17] M. C. Nuss, W. Zinth, and W. Kaiser, "Femtosecond carrier relaxation in semiconductor-doped glasses," *Applied Physics Letters*, vol. 49, no. 25, pp. 1717–1719, 1986.

[18] B. Fluegel, N. Peyghambarian, G. Olbright et al., "Femtosecond studies of coherent transients in semiconductors," *Physical Review Letters*, vol. 59, no. 22, pp. 2588–2591, 1987.

[19] J. L. Coffer, G. Beauchamp, and T. Waldek Zerda, "Porous silica glasses doped with quantum-confined cadmium selenide,"

Journal of Non-Crystalline Solids, vol. 142, no. C, pp. 208–214, 1992.

[20] M. Libbey, "Case presentation: jean," *Psychoanalytic review*, vol. 76, no. 4, pp. 471–509, 1989.

[21] L. L. Hench and J. K. West, "The Sol-Gel process," *Chemical Reviews*, vol. 90, no. 1, pp. 33–72, 1990.

[22] C. J. Brinker and G. W. Scherer, *Sol-Gel Science: The Physics and Chemistry of Sol-Gel Processing*, Academic Press, San Diego, Calif, USA, 1990.

[23] L. Zhang, J. L. Coffer, and T. W. Zerda, "Properties of Luminescent Si Nanoparticles in Sol-Gel Matrices," *Journal of Sol-Gel Science and Technology*, vol. 11, no. 3, pp. 267–272, 1998.

[24] Y. Posada, L. S. Miguel, L. F. Fonseca et al., "Optical properties of nanocrystalline silicon within silica gel monoliths," *Journal of Applied Physics*, vol. 96, no. 4, pp. 2240–2243, 2004.

[25] A. S. Al Dwayyan, M. Naziruddin Khan, and A. A. Ghamdi, "Effect of DCCA on the optical and lasing properties of dye doped Silica gels/ORMOSILs," *Canadian Journal of Pure & Applied Sciences*, vol. 2, no. 1, p. 221, 2008.

[26] M. Naziruddin Khan and A. S. Al Dwayyan, "Influence of solvent on the physical and lasing properties of dye-doped sol-gel host," *Journal of Luminescence*, vol. 128, no. 11, pp. 1767–1770, 2008.

[27] A. S. Al Dwayyan, M. N. Khan, M. S. Al Salhi, A. Al Dukhail, M. S. Al Mansour, and A. A. Al Ghamdi, "Properties of luminescent silicon nanocrystallines doped sol gel for laser applications," *Journal of Materials Science and Engineering*, vol. 3, no. 12, p. 44, 2009.

[28] M. Naziruddin Khan, A. S. Al Dwayyan, M. S. Al Salhi, and M. Al Hoshan, "Study on characteristics of silicon nanocrystals within sol–gel host," *Journal of Experimental Nanoscience*. In press.

[29] M. Nayfeh, O. Akcakir, J. Therrien et al., "Highly nonlinear photoluminescence threshold in porous silicon," *Applied Physics Letters*, vol. 75, no. 26, pp. 4112–4114, 1999.

[30] K. Seino, F. Bechstedt, and P. Kroll, "Influence of SiO_2 matrix on electronic and optical properties of Si nanocrystals," *Nanotechnology*, vol. 20, no. 13, Article ID 135702, 2009.

[31] J. P. Wilcoxon, G. A. Samara, and P. N. Provencio, "Optical and electronic properties of Si nanoclusters synthesized in inverse micelles," *Physical Review B*, vol. 60, no. 4, pp. 2704–2714, 1999.

[32] Z. Ma, X. Liao, G. Kong, and J. Chu, "Absorption spectra of nanocrystalline silicon embedded in SiO_2 matrix," *Materials Letters*, vol. 42, no. 6, pp. 367–370, 2000.

[33] L. Pavesi, "Influence of dispersive exciton motion on the recombination dynamics in porous silicon," *Journal of Applied Physics*, vol. 80, no. 1, pp. 216–225, 1996.

[34] H. Zeng, G. Duan, Y. Li, S. Yang, X. Xu, and W. Cai, "Blue luminescence of ZnO nanoparticles based on non-equilibrium processes: defect origins and emission controls," *Advanced Functional Materials*, vol. 20, no. 4, pp. 561–572, 2010.

[35] N. Daldosso, M. Luppi, S. Ossicini et al., "Role of the interface region on the optoelectronic properties of silicon nanocrystals embedded in SiO_2," *Physical Review B* , vol. 68, no. 8, Article ID 085327, 8 pages, 2003.

[36] A. Fojtik and A. Henglein, "Luminescent colloidal silicon particles," *Chemical Physics Letters*, vol. 221, no. 5-6, pp. 363–367, 1994.

[37] X. Li, Y. He, S. S. Talukdar, and M. T. Swihart, "Process for preparing macroscopic quantities of brightly photoluminescent silicon nanoparticles with emission spanning the visible spectrum," *Langmuir*, vol. 19, no. 20, pp. 8490–8496, 2003.